$NH_4^+ + CH_4$ Gas Phase Collisions as a Possible Analogue to Protonated Peptide/Surface Induced Dissociation†

George L. Barnes and William L. Hase*

Department of Chemistry and Biochemistry, Texas Tech University, Lubbock, Texas 79409

Received: January 31, 2009; Revised Manuscript Received: March 12, 2009

Results are reported for a direct dynamics simulation of $NH_4^+ + CH_4$ gas phase collisions. We interpret the results with protonated peptide/hydrogenated alkanethiolate self-assembled monolayer (H-SAM) surface collisions in mind. Previous theoretical studies of such systems have made use of nonreactive surfaces, and therefore, our goal is to investigate the types and likelihood of peptide/H-SAM reactions. In that vein, the $NH_4^+ + CH_4$ reaction represents a simple gas phase system which includes many of the important interactions present in protonated peptide/H-SAM surfaces. Thirty-seven open pathways are seen in the 5−35 eV collision energy range. An energy dependence on the likelihood of forming CN bonds is found. This type of bonding could deposit both the peptide and its molecular fragments on the H-SAM surface. For our gas phase collision system, around 50% of the trajectories result in the formation of CN bonds. For all collision energies in which reactive scattering occurs, CN bond formation is an important reaction pathway.

1. Introduction

Interfacial interactions influence chemistry in several diverse areas, such as mass spectrometry, atmospheric chemistry, and high-energy combustion reactions. The recent research focus on interfacial chemistry from both an experimental and theoretical standpoint is therefore of no surprise. In the field of mass spectrometry, one area of particular interest involves the collision of a polyatomic ion with a surface. During such events, the ion may dissociatively or nondissociatively scatter, "soft-land," undergo "reactive landing", or become embedded in the bulk. Several studies have been performed involving gas/surface collisions, and in particular, surface-induced dissociation (SID) events, first introduced by Cooks and co-workers,[1] have been extensively studied. SID represents a common technique in mass spectrometry used to fragment and analyze ions colliding with surfaces.[1−5] These types of surface interactions have many similarities to gas phase collisions.

SID has shown great utility in fragmentation of protonated peptides (peptide-H^+).[6−16] High-energy collisions of these peptide-H^+ allows for a relatively rapid and uncomplicated means of determining sequences. Experimentally, energetics and reaction mechanisms of such fragmentation events can be determined by combining SID and electrospray ionization.[17] Computationally, Hase and co-workers[18−28] have made great use of classical trajectory simulations to investigate SID and energy transfer to the surface for a diverse set of systems, including $Si(CH_3)_3^+$, $Cr^+(CO)_6$, and protonated polyglycine and polyalanine. Collisions with both diamond {111} and hydrogenated and perfluorinated alkanethiolate self-assembled monolayers (H-SAM and F-SAM) have been modeled.

Other possibilities in gas/surface collisions are the "soft" and "reactive" landings mentioned briefly above. In such events, the incoming ion remains intact, or nearly intact, and is bound to the surface either physically or chemically. Several nice experimental examples of reactive landing and reactive ion scattering spectrometry are present in the literature.[29−35] Of note is the recent work of Wang et al.[29] in which a close examination of reactive landing is performed. They find a strong dependence on the kinetic energy of the ion for occurrence of reactive landing.

The computational studies mentioned above have focused on SID and energy transfer, not chemical changes to the surface. Therefore, in all the above works, a molecular mechanics (MM) representation of the surface has been utilized. Experimentally, collisions may also induce bond ruptures, chemical reactions, or both, involving atoms of both the surface and peptide-H^+. These products could further dissociate from the surface. A MM treatment of the surface does not allow for these possibilities, and hence, a more flexible treatment is of much interest.

The ideal solution would be a full quantum mechanical treatment of all atoms in the system; however, such an approach is computationally intractable since several thousand atoms are included in models for these systems. Embedding a quantum mechanical region within the top few layers of the surface represents the next step down in sophistication and is a viable option, though still computationally expensive.[36] A smaller and computationally less expensive model for peptide-H^+ colliding with H-SAM type surfaces is the $NH_4^+ + CH_4$ gas phase collision system. The protonated ammonia is analogous to the peptide-H^+, and the methane is analogous to the terminating CH_3 group of the H-SAM surface. Although the collision partners are small, the interactions present are of the same general types that will be present in the large peptide-H^+/H-SAM system. Investigation of the $NH_4^+ + CH_4$ collision system provides insight into both the possibility and types of reactions that may take place between the peptide and the surface. Such insight is important for developing more sophisticated models.

The outline of this paper is as follows. In Section 2, we describe our computational approach. In Section 3, we describe and analyze our trajectory results. In Section 4, we provide a summary.

† Part of the "Robert Benny Gerber Festschrift".

* To whom correspondence should be addressed. E-mail: bill.hase@ttu.edu.

10.1021/jp900919s CCC: $40.75
Published on Web 04/09/2009

TABLE 1: Heats of Formation for Simple Bond Rupture Reactions Calculated with uB3LYP/6-31G(d) and Compared to NIST Values

reaction	NIST[a] (kJ/mol)	uB3LYP/6-31G(d) (kJ/mol)	% difference
$CH_4 \rightarrow CH_3 + H$	438.6	441.6	0.7
$CH_4 \rightarrow CH_2 + 2H$	897.3	911.4	1.6
$CH_4 \rightarrow CH + 3H$	1323.0	1425.8	7.8
$NH_3 \rightarrow NH_2 + H$	454.3	429.	5.6
$NH_2 \rightarrow NH + 2H$	858.5	808.4	5.8

[a] NIST values are from M. W. Chase and are for 298 K.[39]

2. Computational Details

In modeling gas phase $NH_4^+ + CH_4$ collisions, we choose to make use of direct dynamics,[37,38] with the interaction potential calculated using the uB3LYP/6-31G(d) level of theory and basis set. This choice is made on two grounds: First, this combination of level of theory and basis set allows for fast evaluations of the energy gradient and Hessian matrix, which are essential for our chosen direct dynamics method. Second, we find that most of the reaction products in this system result from XH bond rupture, where X is either carbon or nitrogen. A comparison of the heats of formation calculated with uB3LYP/6-31G(d) and NIST[39] values is favorable for a set of basic bond rupture reactions involving CH_4 and NH_3. A summary of these results is displayed in Table 1.

Although the uB3LYP/6-31G(d) energies are not quantitative, they are expected to be sufficiently accurate to give a meaningful description of the $NH_4^+ + CH_4$ reaction dynamics. For the high collision energy simulations reported here, the observed dynamics are expected to be much less sensitive to reaction barrier heights than the kinetics of thermal reactions.[40] For the latter, the reaction rate constant depends exponentially on both the barrier height and temperature. However, for the high-energy $NH_4^+ + CH_4$ collisions, the reaction probabilities are not expected to depend exponentially on either the barrier heights or collision energy.[40] As shown below, indeed, the calculated reaction probabilities are much less sensitive to collision energy than what would be seen for an exponential dependence. A recent example of the relative insensitivity of high-energy simulations to barrier heights are the simulations of protonated glycine, gly-H^+, and surface-induced dissociation with a diamond surface.[19,41] Though the AM1 and MP2/6-31G(d)[19] electronic structure methods yield different energetics for gly-H^+ unimolecular decomposition, they give similar shattering fragmentation dynamics for gly-H^+ when it collides with the diamond surface.

The trajectory calculations were carried out using the general chemical dynamics program VENUS[42] interfaced with the electronic structure theory program NWChem.[43] Initial conditions for each trajectory were selected from a 300K Boltzmann distribution for both rotations and vibrations. The vibrational energy was distributed according to the quasiclassical normal mode method.[44] Both reactants were randomly rotated about their individual centers of mass to sample all relative orientations. The impact parameter was fixed to zero, which is analogous to a normal incident with a surface. The Hessian-based predictor−corrector integration scheme of Lourderaj et al.[45] is utilized.

As described above, the interaction potential is calculated using uB3LYP/6-31G(d). Although the system is closed-shell, a significant radical character is likely in many of the possible reaction pathways because they involve the hydrogen atom. We therefore make use of an open-shell electronic wave function. A small number of trajectories still terminate due to a failure to converge the SCF wave function. However, this is a rare event, and most trajectories had progressed far enough to analyze the results.

A set of trajectories for a range of collision energies from 5 to 35 eV were calculated that conserve energy to within 1 kcal/mol as well as have progressed significantly far down a reaction channel for products to be identified. Each trajectory was run until the carbon and nitrogen are separated by more than 15 Å, an SCF error takes place, or 125 fs of simulation time has passed. At the lowest collision energy, slightly longer simulations were performed to allow the complete separation of products to occur. Trajectories were run in parallel on eight cores and required approximately 1.5 h of wall-clock time. A total of 350 trajectories were calculated, 27 of which are rejected due to energy conservation or SCF failure.

The reaction pathways were determined through use of an in-house code, built upon Open MOPAC7,[46] which determines fragmentation and charge distributions. This code performs single-point PM3 calculations with an unrestricted Hartree−Fock wave function for the final geometry of each trajectory. The electron density is used to construct a "connectivity matrix" which describes the bonding between all atoms. Atoms are considered connected if their bond order is >0.7. This approach has advantages over determination of products solely on the basis of distances because it was seen that on occasion, atoms that would lead to incorrect determination of products could be accidentally close. In particular, this approach allowed for the straightforward determination of 2H from H_2. Charge analysis is performed on individual fragments on the basis of the electron density from the PM3 calculations.

3. Trajectory Results

Our goal is to determine the types and probabilities of reactions occurring between NH_4^+ and CH_4 during gas phase collisions to gain insight into the importance of different types of reactions between a peptide-H^+ and a H-SAM surface. To this end, $NH_4^+ + CH_4$ classical trajectories were propagated with collision energies between 5 and 35 eV.

3.1. Collision Products. For a reactive collision, the most likely events are XH bond ruptures, where X is either carbon or nitrogen. If multiple XH ruptures occur, there are two classes of reaction pathways possible. In the first, two hydrogen atoms interact to form H_2, and in the second, two lone hydrogen atoms are produced. As the number of XH bond ruptures increases, the number of possible pathways increases, as well. If two or more XH ruptures occur, the heavy atoms have two possible classes of reaction pathways, as well. In the first, they impulsively scatter from one another, leading to separated products. In the second, bonds form between the heavy atoms; hence, creating a complex. The combination of the reaction classes for both the hydrogen and heavy atoms, along with multiple XH bond ruptures, leads to a large number of possible reaction pathways. Thirty-seven reaction pathways are open within the 5−35 eV collision energy range and are denoted in Table 2.

In Table 2, the pathways are listed according to the total number of occurrences for all collision energies. The probability for pathways 1−10 are plotted in Figure 1 as a function of collision energy. Note that in some rare cases, partial ($\delta+$) charges are listed. These trajectories terminated before the products were sufficiently separated to force the localization of an electron. If longer trajectories had been performed, such

TABLE 2: Reaction Pathways and Relative Abundance Are Denoted Below[a]

pathway	products	occurrences
1	$NH_4^+ + CH_4$	99
2	$NH_3^+ + CH_3 + 2H$	34
3	$(H_3NCH_3)^+ + H_2$	19
4	$NH_3 + CH_3^+ + H_2$	19
5	$NH_3 + CH_3^+ + 2H$	18
6	$(H_3NCH_3)^+ + 2H$	14
7	$NH_3^+ + CH_2 + 3H$	14
8	$NH_3^+ + CH_3 + H_2$	13
9	$NH_3^+ + CH_2 + H_2 + H$	12
10	$(H_2NCH_2)^+ + 2H_2$	8
11	$NH_3 + CH_2^+ + 3H$	8
12	$NH_2 + CH_3^+ + H_2 + H$	8
13	$(H_2NCH_2)^+ + H_2 + 2H$	7
14	$NH_3 + CH_2^+ + H_2 + H$	7
15	$NH_3^+ + CH_4 + H$	5
16	$NH_2 + CH_2^+ + H_2 + 2H$	5
17	$(H_3NCH_2)^+ + H_2 + H$	4
18	$(H_2NCH_2)^+ + 3H + H$	3
19	$NH_3^{\delta+} + CH_3^{\delta+} + H_2$	3
20	$NH_2^+ + CH_2 + H_2 + 2H$	3
21	$NH_4^+ + CH_2 + H_2$	2
22	$NH_2 + CH_3^+ + 3H$	2
23	$NH + CH_3^+ + 2H_2$	1
24	$NH_2 + CH^+ + H_2 + 3H$	1
25	$NH_4^+ + CH_2 + 2H$	1
26	$(H_3NCH_2)^+ + 3H$	1
27	$NH_2^+ + CH_3 + H_2 + H$	1
28	$NH + CH_2^+ + H_2 + 3H$	1
29	$(H_2NCH_3)^+ + H_2 + H$	1
30	$NH_3^{\delta+} + CH_3^{\delta+} + 2H$	1
31	$NH_3^{\delta+} + CH_2^{\delta+} + H_2 + H$	1
32	$NH_4^+ + CH_3 + H$	1
33	$NH_2 + CH_2^+ + 2H_2$	1
34	$NH_2^+ + CH_2 + 3H + H$	1
35	$NH_2 + CH^+ + 2H_2 + H$	1
36	$NH_2^+ CH + H_2 + 3H$	1
37	$NH_2^+ + CH_3 + 3H$	1

[a] For the products with partial charge, $\delta+$, the trajectories were not integrated long enough to identify the charge localization.

products would not be seen. At the lowest collision energies, no reactive collisions take place. The first reaction pathway to grow in corresponds to formation of $(H_3NCH_3)^+ + H_2$, and at a collision energy of 20 eV, all trajectories result in a reaction. Table 3 reports the reaction pathways for each collision energy with a probability of at least 10% and allows for a quick examination of the character of the dominant pathways. For high collision energies, a wide range of products are seen, and hence, probability is spread among many pathways. The presence of linked pathways involving a low-energy product and a high-energy product is observed. One clear example is pathways 3 and 4. These two products differ only in the presence of a CN bond. At 15 eV, the lower-energy CN complex is dominant, but by 20 eV, the high-energy product is more abundant. Some product pathways also differ solely by H_2 or 2H.

It should be noted that it is possible that the trajectories involving CN bond formation may end up as separated products if the trajectory integration time has increased and unimolecular dissociation of the CN bond has occurred. However, even if this would occur, the presence of these short-lived CN complexes is very important. In collisions with an H-SAM surface, these dissociations are expected to be unimportant because the surface would likely absorb the excess energy. It is well known that surface complexes can lead to new and interesting chemical reactions.

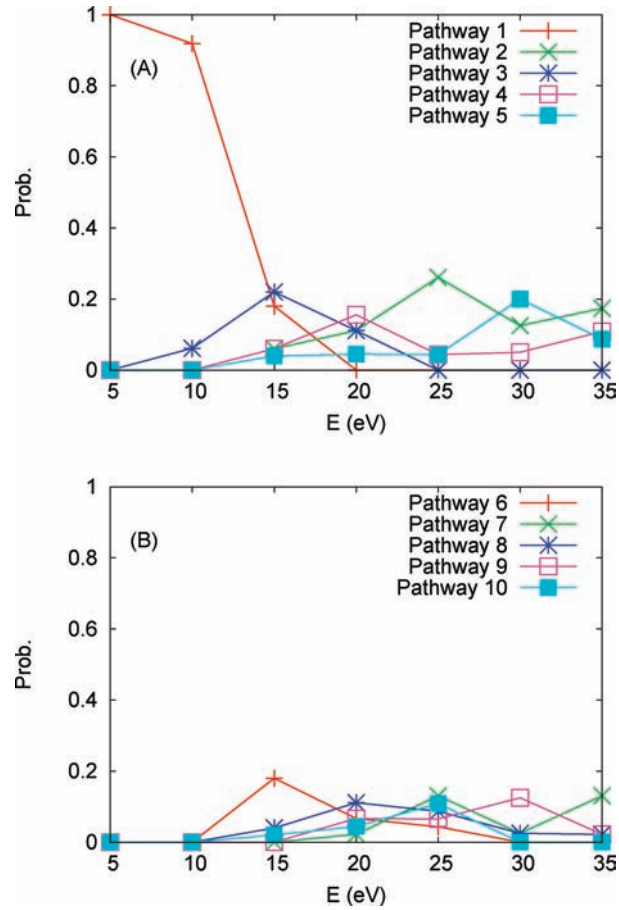

Figure 1. Reaction probabilities for pathways 1−10 as a function of collision energy.

TABLE 3: Reaction Pathways for Each Collision Energy with a Probability >10%

collision energy (eV)	pathway	percentage
5	1	100
10	1	91.8
15	3	22.0
	1	18.0
	6	18.0
20	4	15.6
	2	11.1
	3	11.1
	8	11.1
25	2	26.1
	7	13.0
	10	10.9
30	5	20.0
	2	12.5
	9	12.5
35	2	17.4
	7	13.0
	4	10.9
	11	10.9

If one examines the cumulative probability for all CN bond forming pathways, shown in Figure 2, it is seen that the probability of CN bond formation peaks at 15 eV with a probability of 48%. At high collision energy, the probability drops due to the impulsive nature of high-energy collisions.[18] The number of XH bond ruptures also increases with collision energy as well as the number H atoms produced. Therefore, a competition exists between the energy available for relative translation between the heavy atoms and the energy available for XH bond ruptures, as well as the resulting H atom

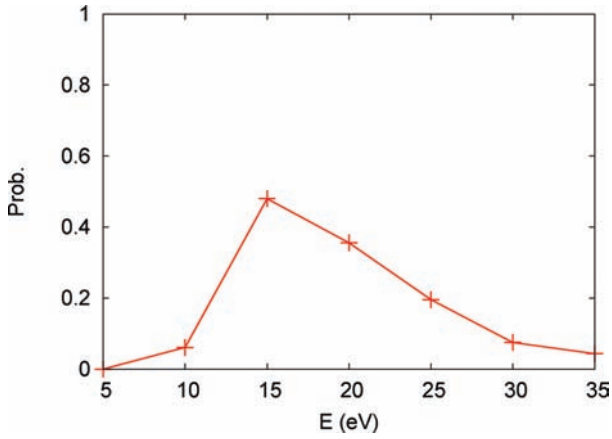

Figure 2. Probability of CN bond formation as a function of collision energy.

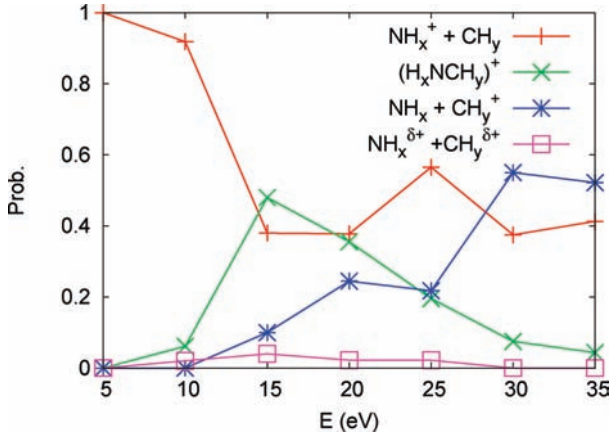

Figure 3. Probability for charge transfer pathways as a function of collision energy.

translations. At the energies considered, the impulsive nature of the collisions dominates this competition, and hence, the decrease in complex formation is seen.

The results from this gas phase system yield intuition concerning the peptide-H^+/H-SAM collision system. On the basis of the above results, two different types of reactions are likely to occur between a peptide-H^+ and the H-SAM surface: The first consists of one or more hydrogen atoms' being removed from the surface and ending as either lone hydrogen(s) or molecular hydrogen. These reactions are probably common because nearly every reactive pathway in our gas phase system involves the removal of at least one hydrogen from methane. The second class of reactions with the H-SAM surface involves formation of a bond between the nitrogen of the peptide and a carbon atom in the surface. The "reactive landing" collisions observed by Laskin and co-workers[29] are similar and in qualitative agreement with our results. However, their SAM is terminated by an ester group, and therefore, a direct comparison is not justified, since chemical reactivity may be important.

3.2. Product Charge Distributions. Our gas phase system has three classes of reaction events: (non)reactive scattering, in which no charge transfer takes place; reactive scattering, in which charge transfer takes place; and CN^+ complex formation. The collision energy dependence of these pathways is shown in Figure 3. At low collision energies, the dominant pathway involves (non)reactive scattering in which the charge remains with the nitrogen. As seen in the previous section, this pathway decreases in probability, though even at our highest collision energies, a fair number of trajectories do not involve charge transfer.

It is of interest that in all trajectories which form a CN complex, the charge is associated with the complex. One very simple explanation for this is that larger atoms/molecules, in general, are more able to stabilize charges. Charge transfer from the nitrogen to the carbon, without complex formation, shows a steady increase, with collision energy. Close to 60% of trajectories following this pathway at high collision energies. As mentioned in the previous section, some of our pathways involve partial charges due to "early" termination of the trajectory. Figure 3 shows that these pathways are a rare occurrence and would not have an effect on the qualitative discussion of charge transfer.

The same types of charge transfer pathways will exist in a peptide-H^+/H-SAM collision. On the basis of the above results in such a system, at low collision energies, little charge transfer should be seen. Toward higher collision energies, many collision events will result in the charge remaining on the surface, either through direct charge transfer or through complexation. However, it must be noted that in such a large system, there are many more ways for the ion to shatter such that the resulting product will retain a charge.

4. Summary

We have presented results of a direct dynamics calculation, making use of the uB3LYP/6-31G(d) model chemistry for the $NH_4^+ + CH_4$ gas phase system, as an analogue to peptide-H^+/H-SAM collisions. Trajectories were calculated for a range of collision energies from 5 to 35 eV. The probability of ending in a given reaction pathway shows a strong energy dependence on the collision energy. Many of the pathways are quite similar and differ only in the amounts of H and H_2 present.

We find that the formation of a CN bond, which is analogous to a peptide bonding to the H-SAM, is probable and important at all reactive collision energies in this study. The probability increases dramatically at 15 eV, with 48% of trajectories forming CN complexes. This probability steadily decreases with increasing collision energy as the impulsive nature of the scattering increases. In our analysis, we have also defined two atoms to be "bonded" if their bond order is >0.7. The quantitative details of the analysis depend on this definition; however, the qualitative conclusions, on which we focus, would remain unchanged for reasonable definitions of a bond.

Our goal is to elucidate the probabilities and types of different reactive scattering events in SID. This information provides useful insight for creating more sophisticated models. This work has shown that reaction with the H-SAM surface is an important possibility and ideally would be included in peptide-H^+/H-SAM models. A molecular mechanics representation of the surface is insufficient, since it does not describe the formation or rupture of bonds between the peptide projective and the surface. Embedding a quantum mechanical region in the H-SAM is a logical first step in future work. A study of the effects of surface stiffness also seems to be warranted. We clearly see that as the collision becomes more impulsive, the probability of CN bond formation decreases. This strongly suggests that as the stiffness of the surface varies, the reactive probability will also be affected. In this work, if we had collided NH_4^+ with CF_4 (i.e., an F-SAM), qualitatively different results would likely have been obtained. Our results suggests that reactions of projectile ions with the surfaces may be an important mechanism for ion loss.[47]

Finally, it is of interest to consider possible differences and similarities in the $NH_4^+ + CH_4$ gas phase and peptide-H^+ +

H-SAM gas−surface reaction dynamics. The $NH_4^+ + CH_4$ collisions are direct, either forming products or scattering nonreactively in ~ 0.1 fs or less. Similar dynamics are found in small peptide-H^+ + H-SAM collisions, which result in a percentage of the collision energy transferred to peptide-H^+ vibration that is independent of the peptide-H^+ size.[18,20] The collisions are impulsive and not complex-forming.[3] The latter would result in collision energy transfer to all of the peptide ion's vibrational modes, with an energy transfer efficiency dependent on the peptide ion's size. An important difference between $NH_4^+ + CH_4$ and peptide-H^+ + H-SAM collisions is the size of the peptide ion and its localized proton. Consider, for example, N-protonated diglycine. If the $-NH_3^+$ moiety collides with a terminal $-CH_3$ group of the H-SAM, reactions as found here for $NH_4^+ + CH_4$ may occur. However, if another region of the glycine ion collides with the H-SAM, there may be no reaction. This effect could be investigated by simulating gas phase collisions of protonated amines, $R-NH_3^+$, with CH_4. A collision of a folded peptide ion, with NH_3^+ in its interior, would be expected to be nonreactive unless the collision unfolds the ion and exposes NH_3^+ so that it interacts with the H-SAM. Even if the $-NH_3^+$ group of the peptide-H^+ collides with the H-SAM, reaction dynamics different from that found here for $NH_4^+ + CH_4$ may result if the collision energy is not principally localized in $-NH_3^+$ and a small region of the H-SAM including a $-CH_3$ group. If this is not the case, there may not be sufficient localization of energy to promote reaction. Software for simulating peptide-H^+ collisions and possible reactions is under development, and in the future, the above questions regarding peptide-H^+ + H-SAM reaction dynamics will be further addressed.[48]

Acknowledgment. This material is based upon work supported by the National Science Foundation under Grants No. OISE-0730114 and CHE-0615321 and the Robert A. Welch Foundation under Grant No. D-0005.

References and Notes

(1) Mabud, M. A.; Dekrey, M. J.; Cooks, R. G. *Int. J. Mass Spectrom. Ion Process.* **1985**, *67*, 285.
(2) McCormack, A. L.; Somogyi, A.; Dongre, A. R.; Wysocki, V. H. *Anal. Chem.* **1993**, *65*, 2859.
(3) Burroughs, J. A.; Wainhaus, S. B.; Hanley, L. *J. Phys. Chem.* **1994**, *98*, 10913.
(4) Kubitsa, J.; Dolejsek, Z.; Herman, Z. *Eur. Mass Spectrom.* **1998**, *4*, 311.
(5) Laskin, J.; Densiov, E.; Futrell, J. *J. Am. Chem. Soc.* **2000**, *122*, 9703.
(6) Jones, J. L.; Dongré, A. R.; Somogi, A.; Wysocki, V. H. *J. Am. Chem. Soc.* **1994**, *116*, 8368.
(7) Cooks, R. G.; Ast, T.; Mabud, M. A. *Int. J. Mass Spectrom. Ion Process.* **1990**, *100*, 209.
(8) Aberth, W. *Anal. Chem.* **1990**, *62*, 609.
(9) Bier, M. E.; Schwartz, J. C.; Schey, K. L.; Cooks, R. G. *Int. J. Mass Spectrom. Ion Process.* **1990**, *103*, 1.
(10) Williams, E. R.; Henry, K. D.; McLafferty, F. W.; Shabanowitz, J.; Hunt, D. F. *J. Am. Soc. Mass Spectrom.* **1990**, *1*, 413.
(11) Cole, R. B.; Lemeillour, S.; Tabet, J. C. *Anal. Chem.* **1992**, *64*, 365.
(12) McCormack, A. L.; Jones, J. L.; Wysocki, V. H. *J. Am. Soc. Mass Spectrom.* **1992**, *3*, 859.
(13) Wright, A. D.; Despeyroux, D.; Jennings, K. R.; Evans, S.; Riddoch, A. *Org. Mass Spectrom.* **1992**, *27*, 525.
(14) Meot-Ner, M.; Dongré, A. R.; Somogyi, Á.; Wysocki, V. H. *Rapid Commun. Mass Spectrom.* **1995**, *9*, 829.
(15) Chorush, R. A.; Little, D. P.; Beu, S. C.; Wood, T. D.; McLafferty, F. W. *Anal. Chem.* **1995**, *67*, 1042.
(16) Schey, K. L.; Durkin, D. A.; Thornburg, K. R. *J. Am. Soc. Mass Spectrom.* **1995**, *6*, 257.
(17) Dongré, A. R.; Somogyi, Á.; Wysocki, V. H. *J. Am. Chem. Soc.* **1996**, *118*, 8365.
(18) Yang, L.; Mazyar, O. A.; Lourderaj, U.; Wang, J.; Rodgers, M. T.; Martinez-Nunez, E.; Addepalli, S. V.; Hase, W. L. *J. Phys. Chem. C* **2008**, *112*, 9377–9386.
(19) Park, K.; Song, K.; Hase, W. L. *Int. J. Mass Spectrom.* **2007**, *265*, 326.
(20) Rahaman, A.; Zhou, J. B.; Hase, W. L. *Int. J. Mass Spectrom.* **2006**, *249−250*, 321.
(21) Rahaman, A.; Collins, O.; Scott, C.; Wang, J.; Hase, W. L. *J. Phys. Chem. A* **2006**, *110*, 8418.
(22) Wang, J.; Meroueh, S. O.; Wang, Y.; Hase, W. L. *Int. J. Mass Spectrom.* **2003**, *230*, 57.
(23) Wang, Y.; Hase, W. L.; Song, K. *J. Am. Soc. Mass Spectrom.* **2003**, *14*, 1402.
(24) Song, K.; Meroueh, O.; Hase, W. L. *J. Chem. Phys.* **2003**, *118*, 2893.
(25) Meroueh, O.; Hase, W. L. *J. Am. Chem. Soc.* **2002**, *124*, 1524.
(26) Meroueh, O.; Hase, W. L. *Phys. Chem. Chem. Phys.* **2001**, *3*, 2306.
(27) Bosio, S. B. M.; Hase, W. L. *Int. J. Mass Spectrom. Ion Process.* **1998**, *174*, 1.
(28) Schultz, D. G.; Wainhaus, S. B.; Hanley, L.; de Sainte Claire, P.; Hase, W. L. *J. Chem. Phys.* **1997**, *106*, 10337.
(29) Wang, P.; Hadjar, O.; Gassman, P. L.; Laskin, J. *Phys. Chem. Chem. Phys.* **2008**, *10*, 1512.
(30) Volny, M.; Elam, W. T.; Ratner, B. D.; Turecek, F. *Anal. Chem.* **2005**, *77*, 4846.
(31) Volny, M.; Elam, W. T.; Branca, A.; Ratner, B. D.; Tureek, F. *Anal. Chem.* **2005**, *77*, 4890.
(32) Luo, H.; Miller, S. A.; Cooks, R. G.; Pachuta, S. J. *Int. J. Mass Spectrom.* **1998**, *174*, 193.
(33) Smith, D. L.; Selvan, R.; Wysocki, V. H. *Langmuir* **2003**, *19*, 7302–7306.
(34) Angelico, V. J.; Mitchell, S. A.; Wysocki, V. H. *Anal. Chem.* **2000**, *72*, 2603–2608.
(35) Gu, C.; Wysocki, V. H.; Harada, A.; Takaya, H.; Kumadaki, I. *J. Am. Chem. Soc.* **1999**, *121*, 10554–10562.
(36) Li, G.; Bosio, S. B. M.; Hase, W. L. *J. Mol. Struct.* **2000**, *556*, 43–57.
(37) Bolton, K.; Hase, W. L.; Peslherbe, G. H. In *Modern Methods for Multidimensional Dynamics Computations in Chemistry*; Thompson, D. L., Ed.; World Scientific: Singapore, 1998; p 143.
(38) Sun, L.; Hase, W. L. *Rev. Comput. Chem.* **2003**, *19*, 79.
(39) Chase, M. W., Jr. *J. Phys. Chem. Ref. Data, Monograph* **1998**, *9*, 1–1951.
(40) Levine, R. D.; Bernstein, R. B. *Molecular Reaction Dynamics and Chemical Reactivity*; Oxford: New York, 1987.
(41) Meroueh, S. O.; Wang, Y.; Hase, W. L. *J. Phys. Chem. A* **2002**, *106*, 9983.
(42) (a) Hase, W. L.; Duchovic, R. J.; Hu, X.; Komornicki, A.; Lim, K. F.; Lu, D. H.; Peslherbe, G. H.; Swamy, K. N.; Vande Linde, S. R.; Varandas, A. J. C.; Wang, H.; Wolf, R. J. *Quant. Chem. Prog. Exch. (QCPE) Bull.* **1996**, *16*, 671. (b) Hu, X.; Hase, W. L.; Pirraglia, T. *J. Comput. Chem.* **1991**, *12*, 1014.
(43) Kendall, R. A.; Aprá, E.; Bernholdt, D. E.; Bylaska, E. J.; Dupuis, M.; Fann, G. I.; Harrison, R. J.; Ju, J.; Nichols, J. A.; Nieplocha, J.; Straatsma, T. P.; Windus, T. L.; Wong, A. T. *Comput. Phys. Commun.* **2000**, *128*, 260–283.
(44) Peslherbe, G. H.; Wang, H.; Hase, W. L. *Adv. Chem. Phys.* **1999**, *105*, 171–201.
(45) Lourderaj, U.; Song, K.; Windus, T. L.; Zhuang, Y.; Hase, W. L. *J. Chem. Phys.* **2007**, *126*, 044105.
(46) A GPL program freely avaiable from http://www.openmopac.net. (Accessed, April 3, 2009).
(47) Somogyi, A.; Kane, T. E.; Ding, J. M.; Wysocki, V. H. *J. Am. Chem. Soc.* **1993**, *115*, 5275–5283.
(48) Barnes, G. L.; Hase, W. L. work in progress.

JP900919S